Chapter 4

Dielectric and Mechanical Properties of $CaCu_3Ti_4O_{12}$/ Poly(vinylidene fluoride) Composites

The present chapter describes the structural, dielectric and mechanical behavior of $CaCu_3Ti_4O_{12}$ / PVDF (PVDF-CCTO) composites. $CaCu_3Ti_4O_{12}$ has been prepared by solid state conventional method. CCTO in varying amount viz 10, 20 and 50 wt% has been dispersed in PVDF matrix to prepare the composites. Composites are prepared by melt extrusion process. The effect of variation of CCTO content on the above properties has been reported. It is found that CCTO dispersion in PVDF improves the thermal, dielectric and mechanical properties of the composites.

4. Results and discussion

4.1. Structural Analysis

X-ray diffraction patterns of the CCTO, PVDF and the composites containing 10, 20 and 50 wt % CCTO (PVDF-CCTO) are shown in Fig 4.1. Formation of the single phase CCTO has been confirmed by powder X-ray diffraction (XRD) using CuKα radiation. In the case of CCTO, the diffraction peaks corresponding to the planes (220), (310), (222), (321), (400), (422) and (440) are observed at 2θ values of 34.2°, 38.5°, 42.3°, 45.8°, 49.2°, 61.3° and 72.2° respectively. This confirms the formation of single phase CCTO [Sinclair et al (2002)]. There is no evidence of any secondary phase in CCTO.

α- PVDF has been used in the present work (as supplied). This is proved by its characteristic 2θ peaks at 17.7°, 18.7°and 19.9° corresponding to (100), (020) and (110) reflections respectively [Varma et al (2010)]. Intensity of the three major peaks (220), (400) and (422) of CCTO in the composites increases with its increasing amount. Predominance of CCTO phase can be seen in the XRD pattern of PVDF-50CCTO. This is indicated by the suppression of the peaks of PVDF. In CCTO, (220), (400) and (422)

peaks are present at 34.2°, 49.2° and 61.3° which shift to 34.7°, 49.7° and 61.8° respectively in the case of PVDF-50CCTO. This shift in the peaks towards higher 2θ values is due to a decrease in the interplanar spacing. Compression of CCTO particles by PVDF matrix may lead to decrease in the interplanar spacing.

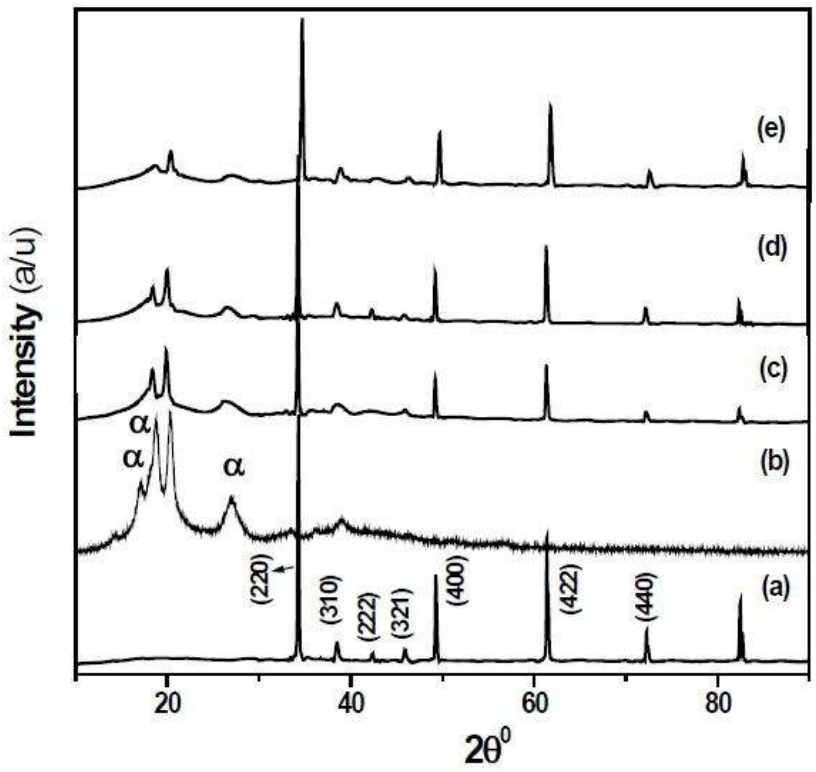

Figure 4.1 X-ray diffraction patterns for (a) CCTO, (b) PVDF, (c) PVDF-10CCTO, (d) PVDF-20CCTO and (e) PVDF-50CCTO composites.

4.2. Surface morphology

Distribution of ceramic particles in the polymer matrix plays an important role in determining the properties of the composite materials. Figure 4.2 shows SEM micrographs of PVDF and the composites. Pure PVDF exhibits spherulitic morphology. It is observed that the spherulitic morphology of pure PVDF is significantly changed by dispersion of CCTO powder. Figure 4.2 shows that ceramic particles are well dispersed in the polymer matrix for low concentration of CCTO. As the filler concentration

increases, inter - particle distance decreases, leading to the formation of a connected network structure. This is evident from the SEM micrograph of the PVDF-50CCTO sample. These changes in the morphology of the composites influence the properties. This well connected network structure in PVDF-50CCTO gives rise to an enhanced ε' and improved mechanical properties as described below.

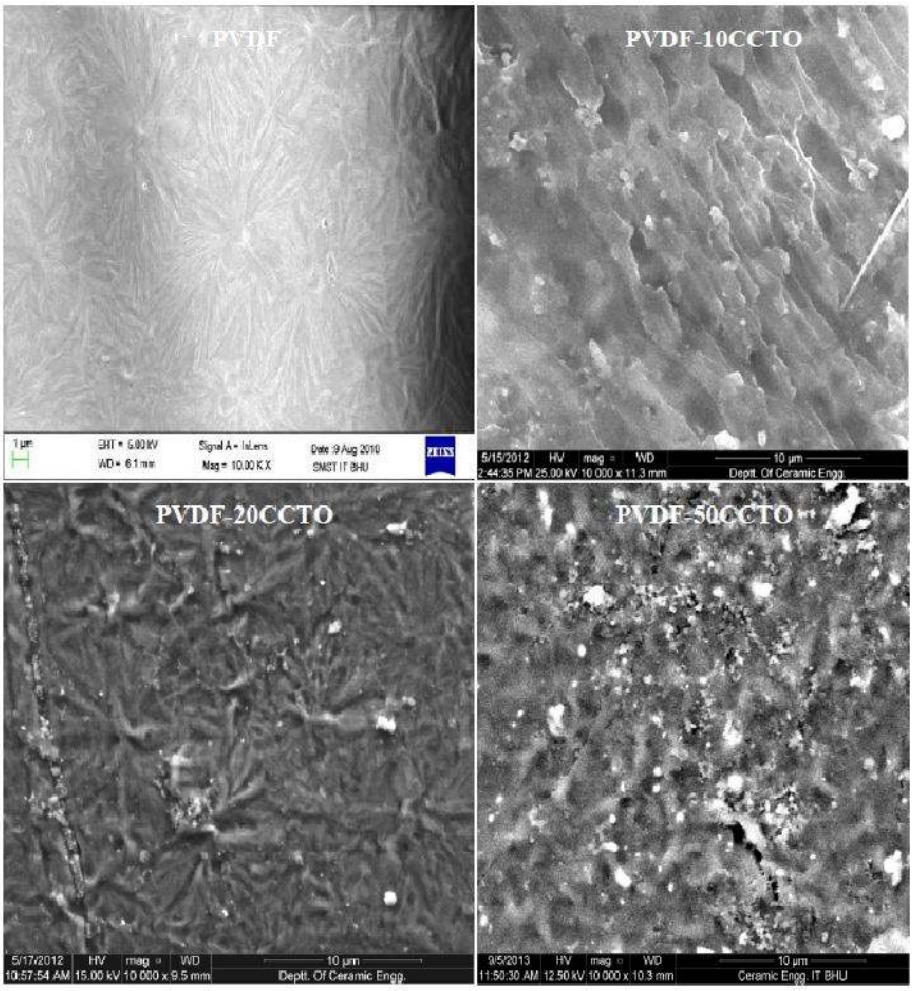

Figure 4.2 Scanning electron micrographs of PVDF, PVDF-10CCTO, PVDF-20CCTO and PVDF-50CCTO composites

4.3. Thermal behavior

Thermogravimetric analysis (TGA) has been carried out to study the thermal stability of the polymer and the composites. Thermograms recorded for the pure PVDF and its composites are shown in Fig 4.3. It is observed that pure PVDF is stable up to 400°C and complete degradation of the polymer occurs around 500°C. Addition of CCTO ceramic filler influences the thermal decomposition behavior of PVDF. CCTO filler shifts the degradation temperature to higher side i.e. from 442^0C in PVDF to 442^0C, 456^0C and 464^0C in PVDF-10CCTO, PVDF-20CCTO and PVDF-50CCTO respectively. It shows that addition of CCTO improves the thermal stability of the composites.

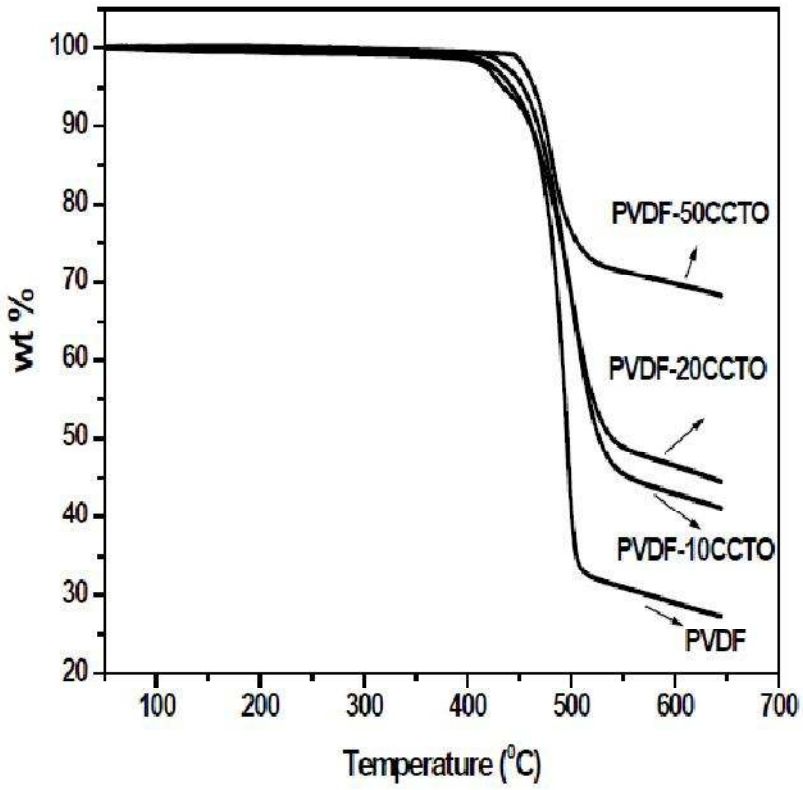

Figure 4.3 TGA of PVDF, PVDF-10CCTO, PVDF-20CCTO and PVDF-50CCTO composites.

4.4. Mechanical properties

Figure 4.4 (a) shows the stress-strain curves of PVDF and the composites. Three samples are tested for each composition and average is taken. Considerable increase has been observed in the Young's modulus which is calculated from the slope of the linear region of the plots. For PVDF, PVDF-10CCTO, PVDF-20CCTO and PVDF-50CCTO, values of the Young's modulus are 750, 770, 865 and 960 MPa respectively (Fig 4.4 b). Elongation at breaking point decreases from 30% in PVDF to 21%, 19% and 16% in PVDF-10CCTO, PVDF-20CCTO and PVDF-50CCTO composites respectively (Fig 4.4 c). This increase in the Young's modulus with filler content can be attributed to increase in the resistance to the free movement of the polymeric chains by much harder ceramic particles. This also explains the observed decrease in the elongation at the breaking point with increasing concentration of ceramic in the PVDF matrix.

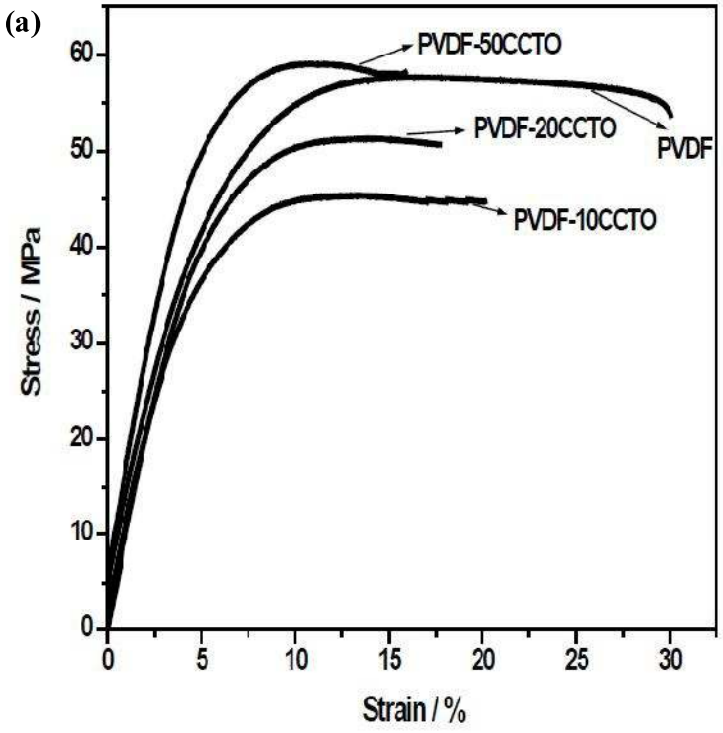

Figure 4.4 (a) Stress-strain curves for the pure PVDF, PVDF-10CCTO, PVDF-20CCTO and PVDF-50CCTO composites,

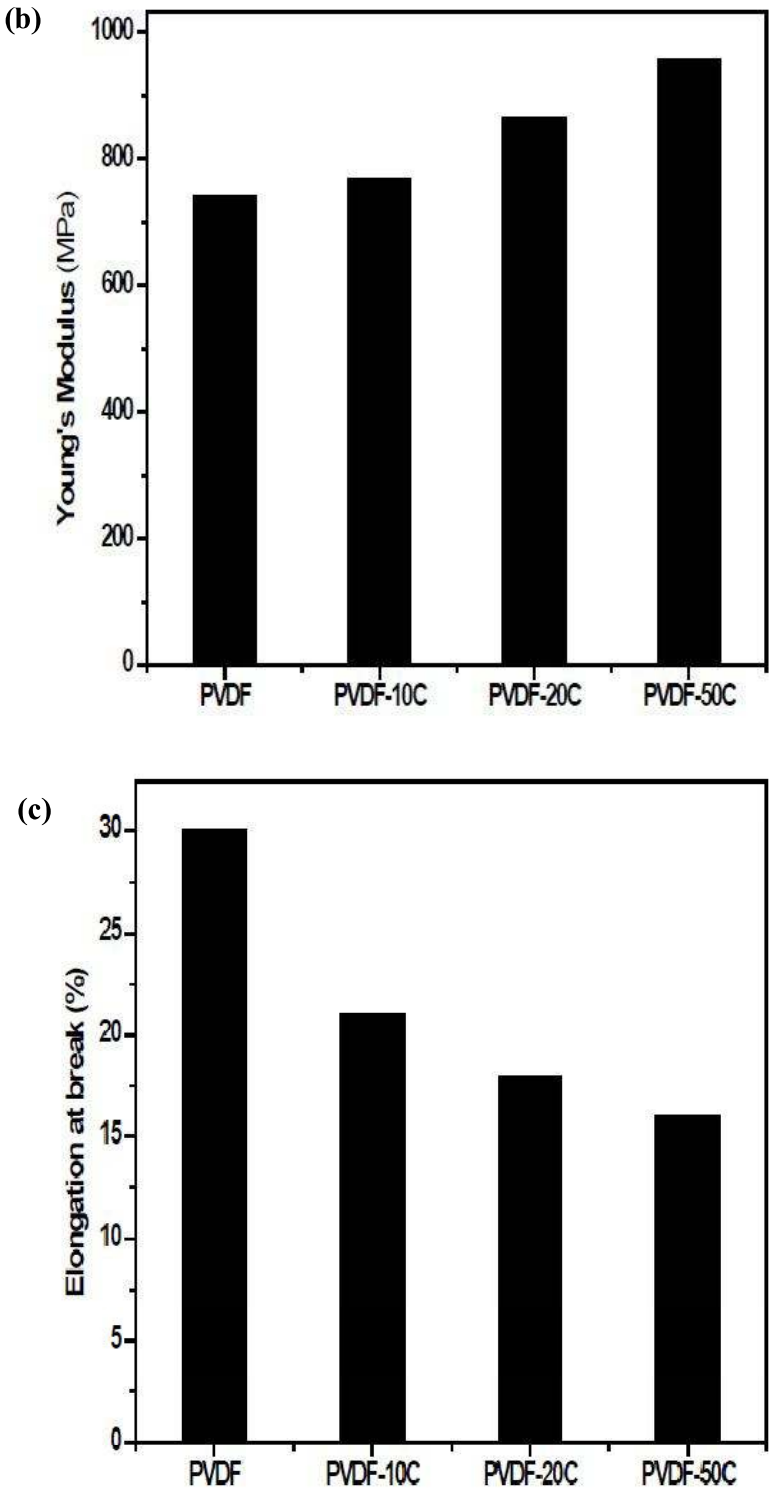

Figure 4.4 (b) Young's modulus of PVDF and the composites and (c) Elongation at the breaking point of PVDF and composites.

4.5. Dielectric properties

Frequency dependence of the dielectric permittivity and tan δ of CCTO, PVDF and the composites is shown in figs 4.5 (a-k). At 40°C and 100 Hz, dielectric permittivity (ε') of CCTO is 3100. It is observed from the fig 4.5(a) that ε' is independent of frequency in the frequency range 1 Hz to 10^6 Hz. The giant permittivity of CCTO depends on the microstructure and on the formation of the internal boundary layer capacitors (IBLC) between the grains [Sinclair et al (2002)]. ε' increases with temperature in PVDF, it is 3 at 40^0C and 100 Hz which increases to 8 at 120^0C and 100 Hz (Fig 4.5 b). For PVDF ε' is 3.0, which increases to 11, 15 and 53 for PVDF-10CCTO, PVDF-20CCTO and PVDF-50CCTO respectively at 100 Hz and 40^0C (Fig 4.5 d). PVDF is present in α phase, which is non-polar. Due to the non-polar nature of PVDF, ε' is low for PVDF. The dielectric permittivity of the composites is more than that of PVDF throughout the frequency range studied. ε' increases with the increase in CCTO content. It decreases with increase in the frequency and increases with temperature (Figs 4.5 b, f, h and j). The high ε' of the composites is mainly because of the interfacial polarization and high dielectric permittivity of the ceramic filler used. Initially there is rapid decrease in ε' with frequency and then it becomes constant after a particular frequency. It is observed from figs 4.5 (f, h and j) that the frequency after which ε' becomes constant shifts to higher side with increasing CCTO. This is characteristic of the interfacial or space charge polarization. Interfacial polarization is always present in the composites because of the difference in the conductivity of the dispersed phase (CCTO in this case) and the matrix (PVDF in this case). The charge moves through the CCTO but get intercepted at the polymer-ceramic interface giving rise to giant dipoles. These give rise to high value of ε'. These giant dipoles cannot follow alterations in the electric field leading to decrease in ε' with increasing frequency.

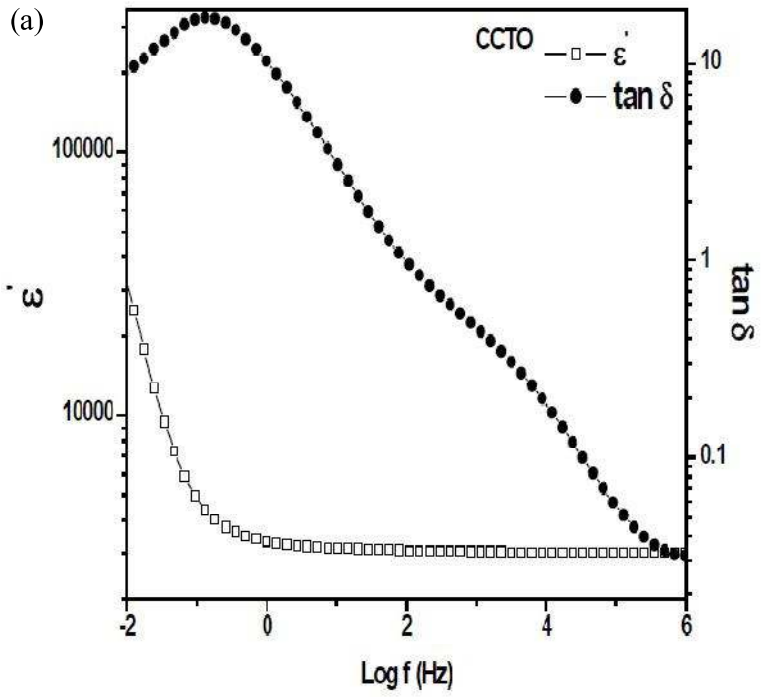

Figure 4.5 Frequency dependence of dielectric permittivity and tan δ of (a) CCTO at 40^0C.

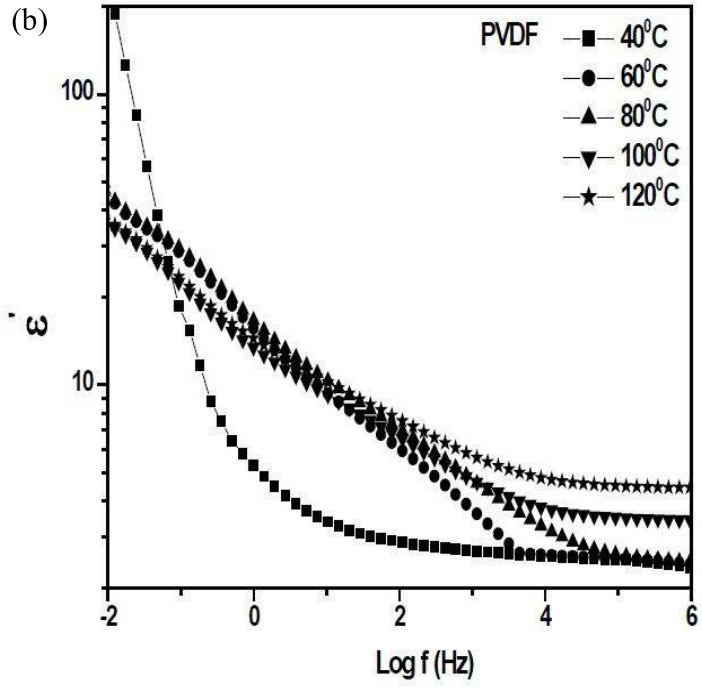

Figure 4.5 (b) Frequency dependence of dielectric permittivity of PVDF at different temperatures

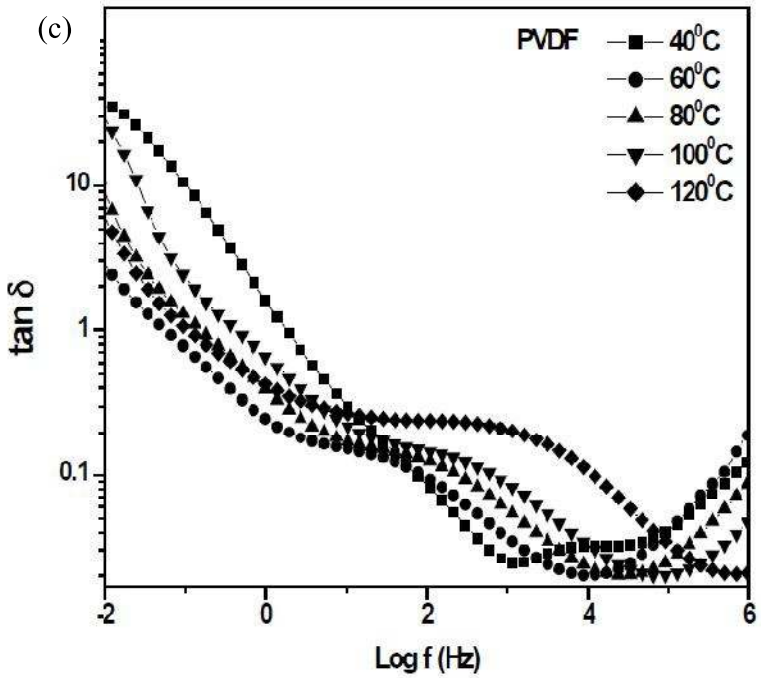

Figure 4.5 (c) Frequency dependence of tan δ of PVDF at different temperatures.

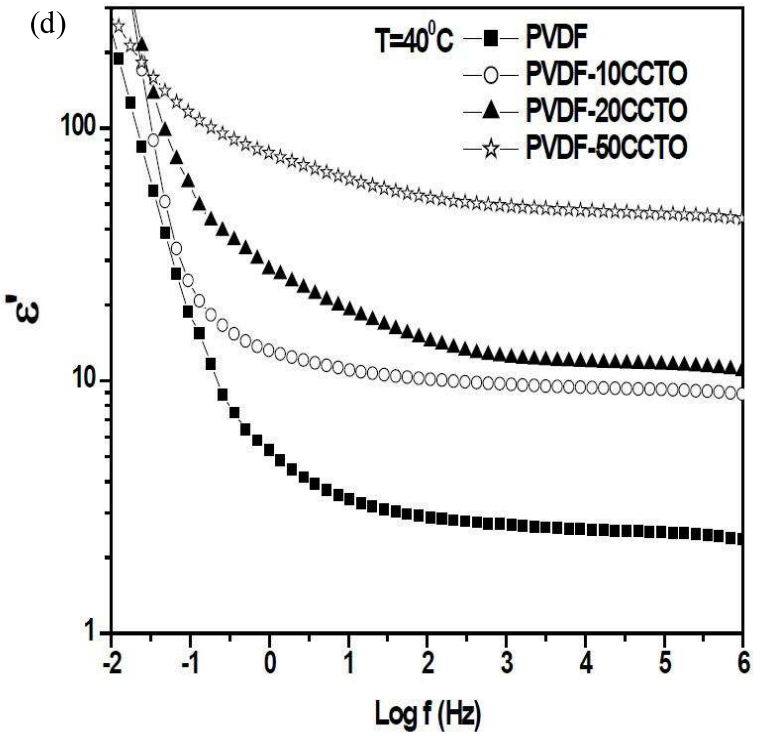

Figure 4.5 (d) Frequency dependence of dielectric permittivity of PVDF and all the composites at 40^0 C.

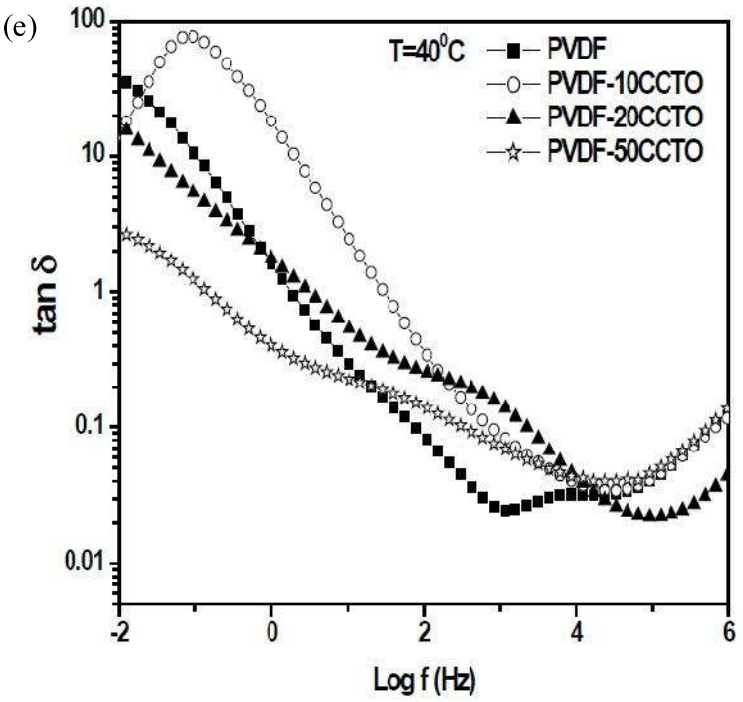

Figure 4.5 (e) Frequency dependence of tan δ of PVDF and all the composites at 40^0 C.

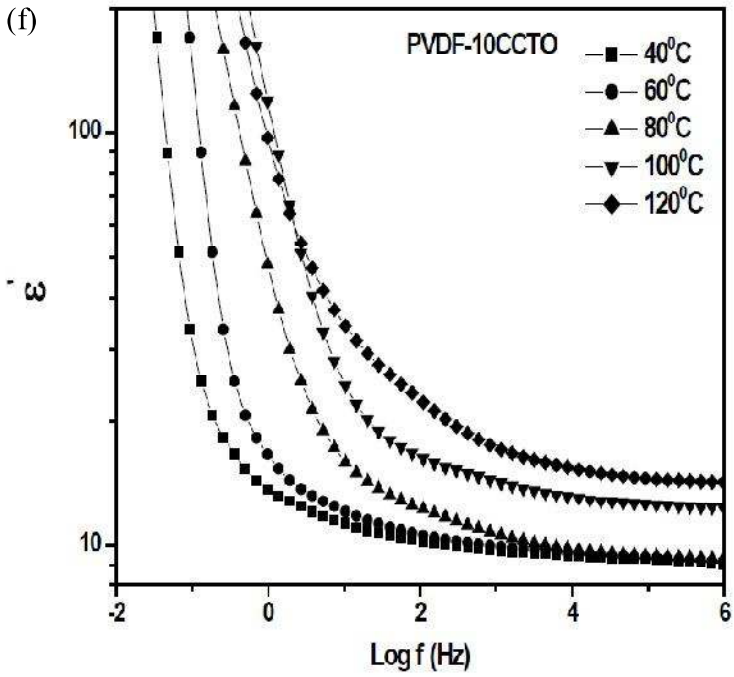

Figure 4.5 (f) Frequency dependence of dielectric permittivity of PVDF-10CCTO at different temperatures

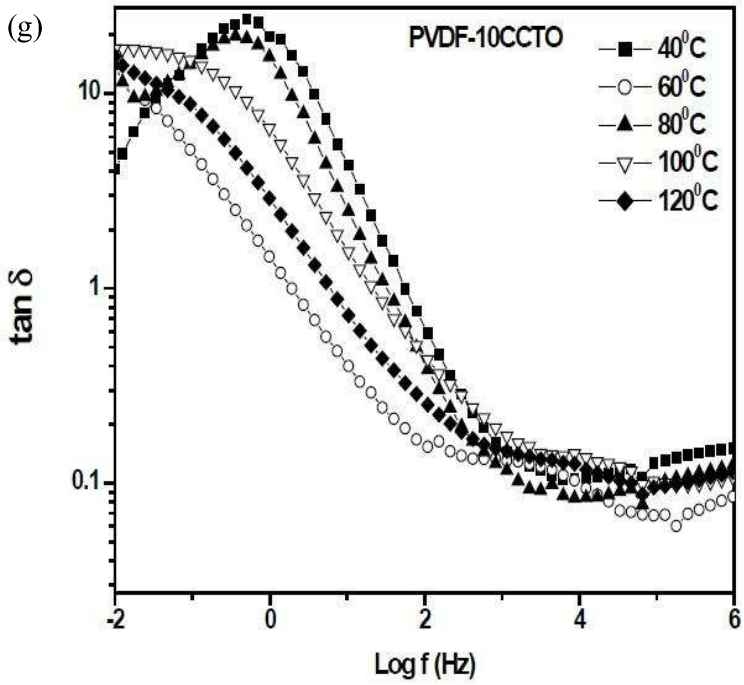

Figure 4.5 (g) Frequency dependence of tan δ of PVDF-10CCTO at different temperatures

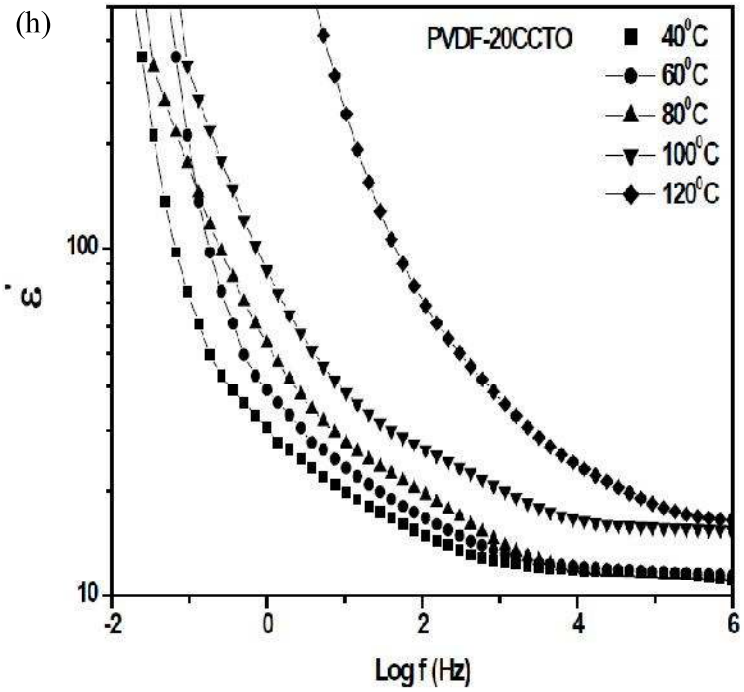

Figure 4.5 (h) Frequency dependence of dielectric permittivity of PVDF-20CCTO at different temperatures.

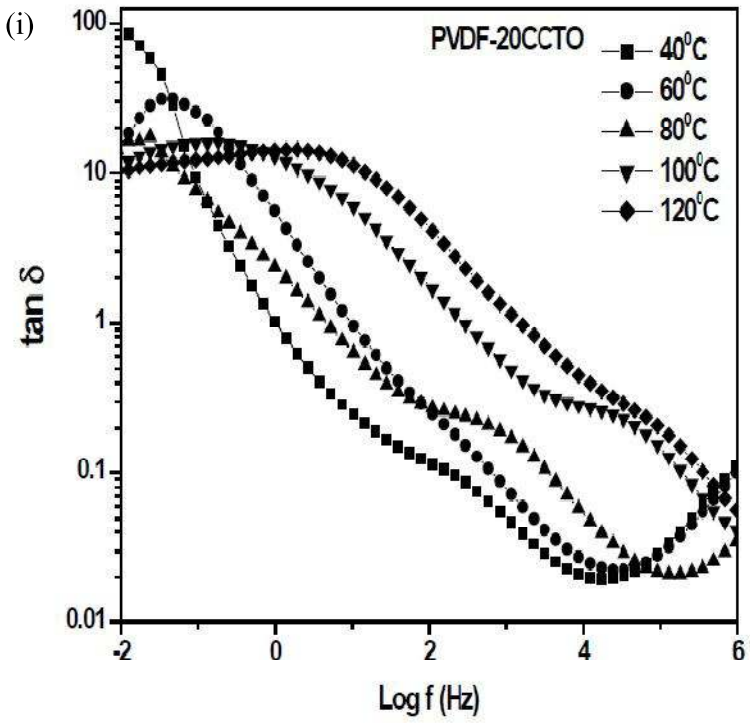

Figure 4.5 (i) Frequency dependence of tan δ of PVDF-20CCTO at different temperatures.

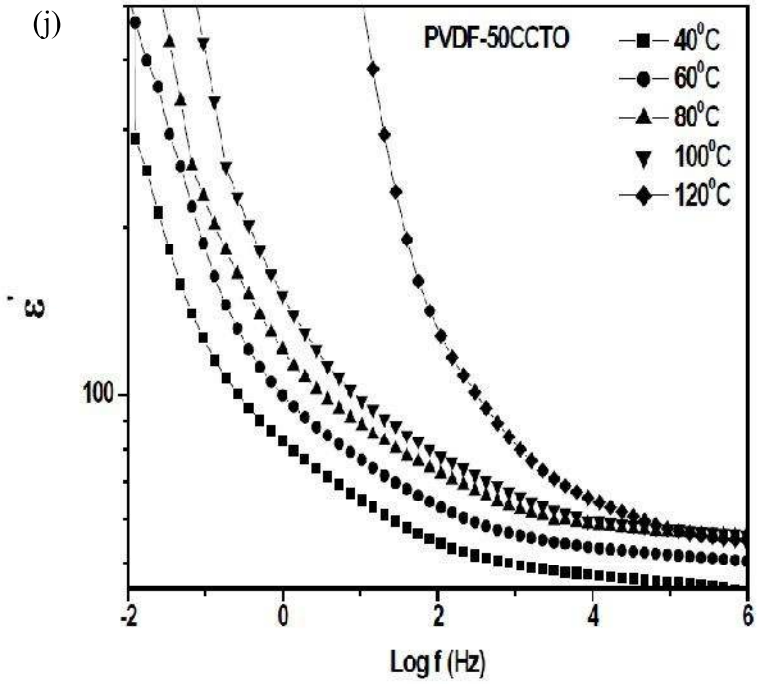

Figure 4.5 (j) Frequency dependence of dielectric permittivity of PVDF-50CCTO at different temperatures.

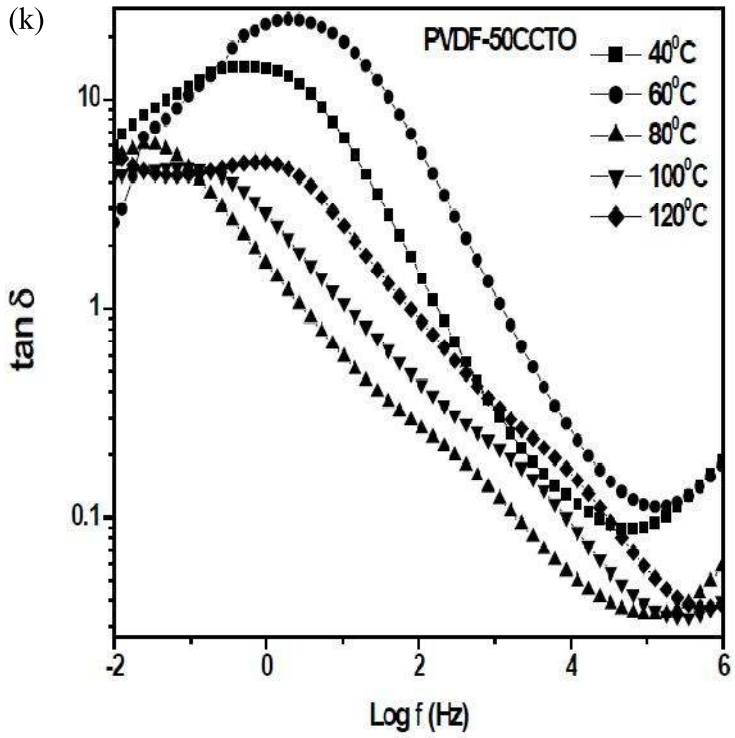

Figure 4.5 (k) Frequency dependence of tan δ of PVDF-50CCTO at different temperatures.

The dielectric loss (tan δ) of CCTO at 40°C and 100 Hz is 0.9 (Fig 4.5 a). The dielectric loss increases with decrease in frequency. This is due to dc conductivity. In CCTO, one relaxation appears in the low frequency range and other in the intermediate frequency range (10^3-10^4Hz) (Fig 4.5 a). Tan δ at 40^0C and 100 Hz, for PVDF, PVDF-10CCTO, PVDF-20CCTO and PVDF-50CCTO is 0.08, 0.14, 0.26 and 0.34 respectively (Fig 4.5 e). It is has been reported that the loss tangent values are high at low frequencies up to 1 kHz and at frequency more than 1 MHz [Sinclair et al (2002)]. It remains low in the frequency range 10 kHz to 1 MHz.

In the case of PVDF-CCTO composites, one relaxation appears at lower frequency (0.1Hz), and other appears at ~100 Hz (Figs 4.5 g, i and k). Relaxation at lower frequency can be attributed to Maxwell Wagner polarization in the composites and the one in the intermediate frequency range can be attributed to α_c relaxation associated with molecular motion of the polymer chains in the crystalline regions of PVDF. The glass

transition relaxation α_a of PVDF occurs beyond 1 MHz (Fig 4.5 c) [Gregoria and Cestari (1994); Gregoria and Ueno (1999); Channel and Jog (2008)]. These relaxation peaks shift to higher frequency with increase in temperature indicating lower relaxation time (τ). This seems to be due to the ease of relaxation because of decrease in the viscosity of the polymer with temperature.

To understand the nature of dielectric relaxation, use is made of modulus spectroscopy. Electrical modulus is defined as the inverse of the complex permittivity.

$$M^* = \frac{1}{\varepsilon^*} = \frac{1}{(\varepsilon' - J\varepsilon'')} = \frac{\varepsilon'}{(\varepsilon'^2 + \varepsilon''^2)} + \frac{J\varepsilon''}{(\varepsilon'^2 + \varepsilon''^2)} = M' + J.M'' \qquad (4.1)$$

where M', ε', and M", ε" are the real and the imaginary parts of the modulus and permittivity respectively. On dispersing CCTO in PVDF (Fig 4.6 a), the value of M' decreases. This implies an increase in ε' with the ceramic content. Variation of M" with temperature for PVDF is shown in fig 4.6 (b). Fig 4.6 (c) shows variation of imaginary part of the electrical modulus (M") at various temperatures as a function of frequency for the composites. It is evident from the figure that with ceramic dispersion in PVDF matrix, the maximum value of M" decreases. Two relaxations can be observed in the M" vs log f plots of composites.

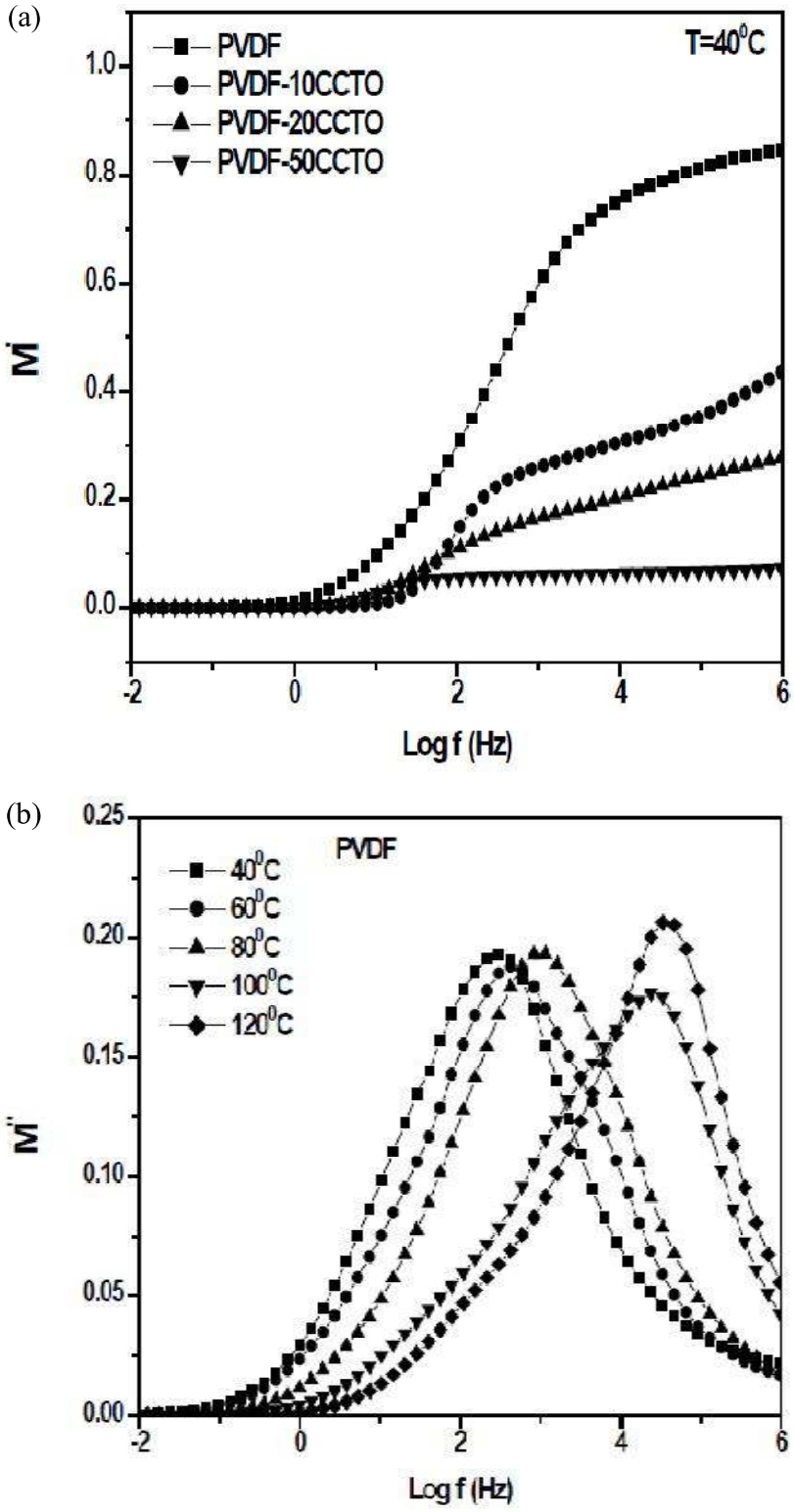

Figure 4.6 (a) M' vs log f plots of PVDF and composites at 40^0 C, (b) M'' vs log f plots of PVDF at different temperatures

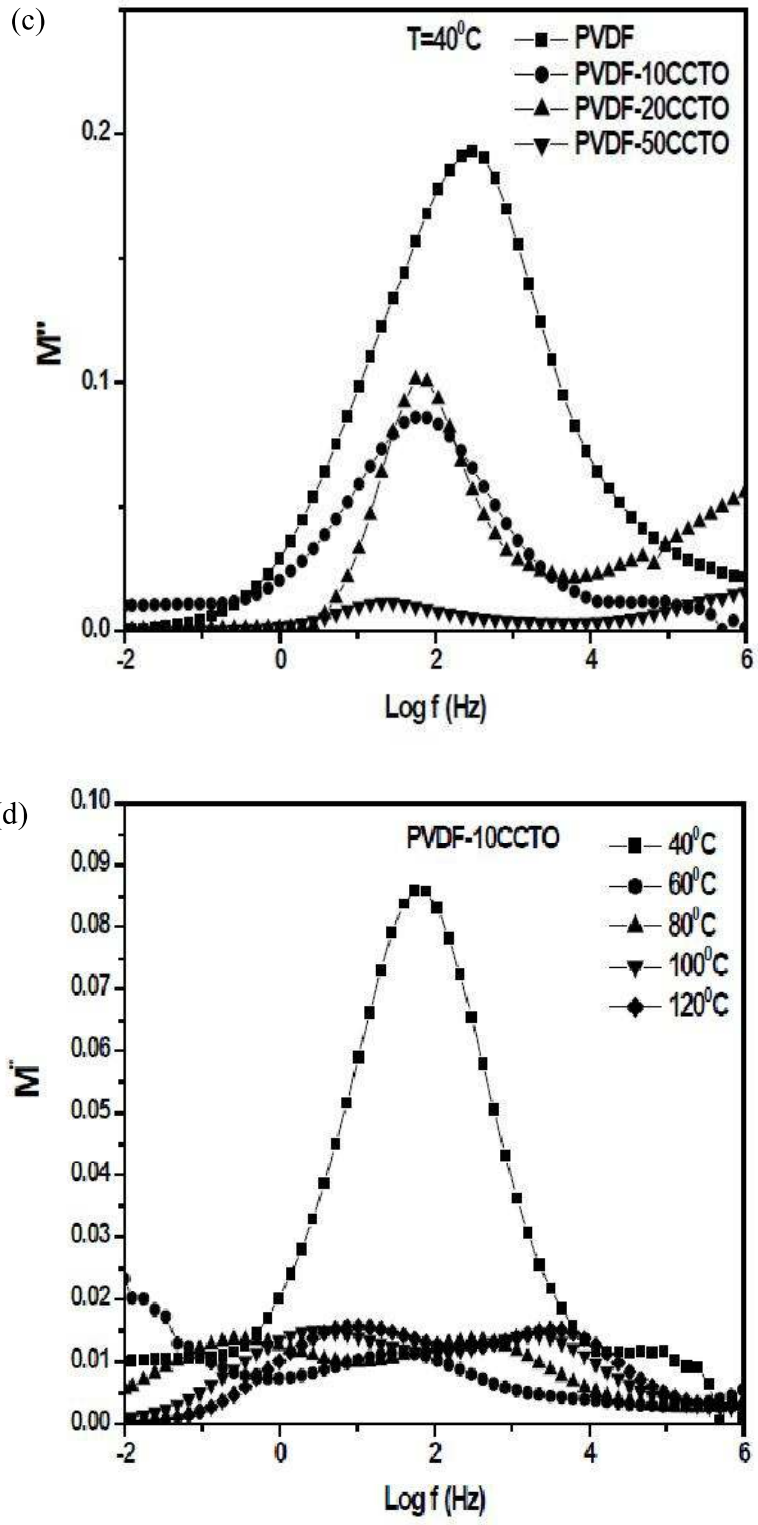

Figure 4.6 M" vs log f plots of (c) PVDF and PVDF-CCTO composites at 40^{0}C, (d) PVDF-10CCTO at different temperatures.

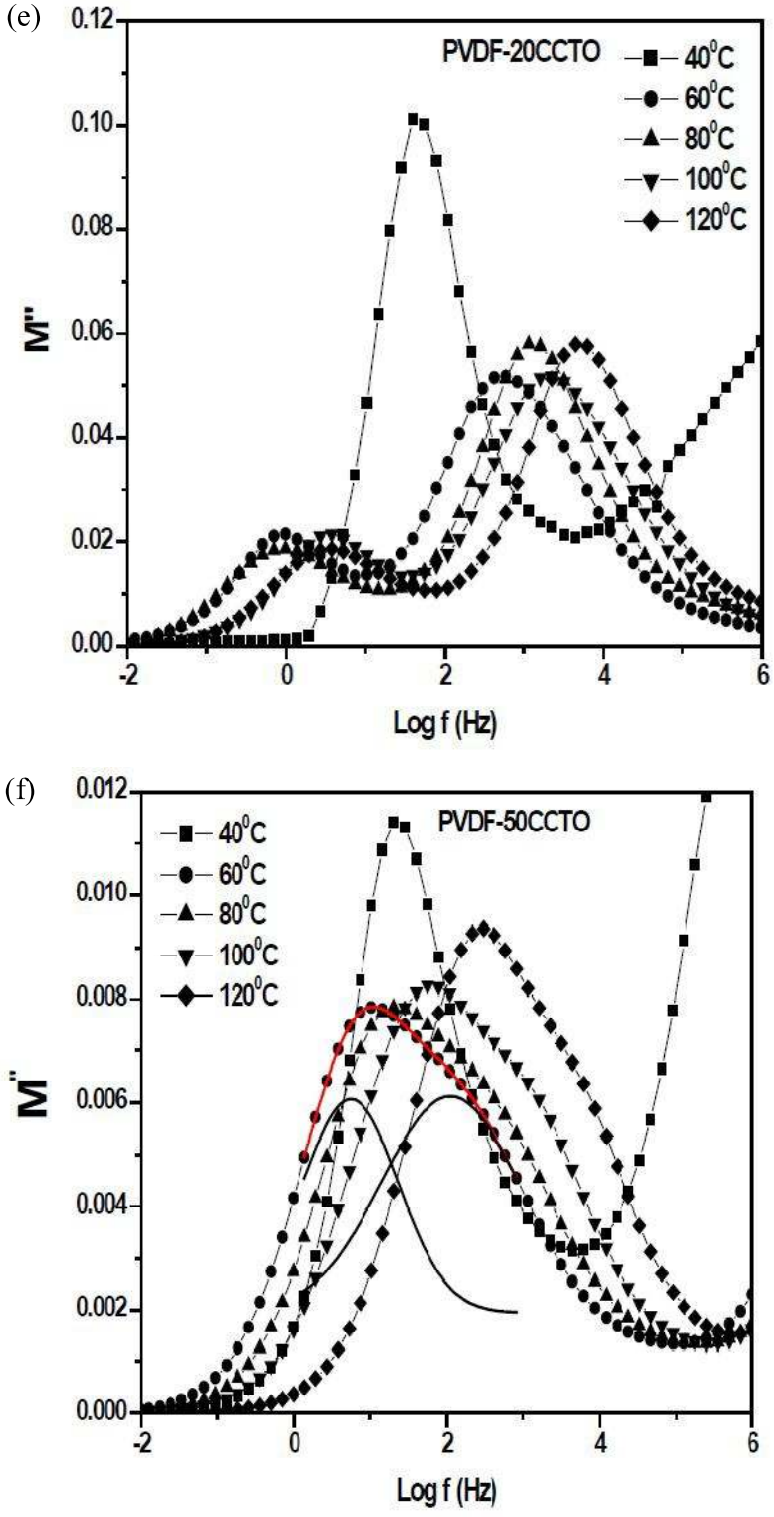

Figure 4.6 M" vs log f plots of (e) PVDF-20CCTO at different temperatures and (f) PVDF-50CCTO at different temperatures.

Fig 4.6 (c) shows M" vs log f plots of PVDF, PVDF-10CCTO, PVDF-20CCTO and PVDF-50CCTO at 40^0C. It is noted that one relaxation appears in PVDF as well as in the composites around 100 Hz. This relaxation is due to α_c relaxation associated with molecular motion of the polymer chains in the crystalline regions of PVDF. It is observed that this relaxation peak shifts to lower frequency in composites with the increase in CCTO content. This is due to restricted mobility of the polymeric chains because of their interaction with the stiff filler particles. Height of the peak is less in the case of the composites. This shows that the dielectric permittivity as well as the dielectric loss is more in the composites as compared to that in pure PVDF. These peaks shift to higher frequency with increasing temperature.

In the composites, another peak appears at low frequency and high temperature (above 60^0C) in the case of PVDF-10CCTO and PVDF-20CCTO (Figs 4.6 d-e). In PVDF-50CCTO, the low frequency peak in M" merges with the peak due to molecular motion of the polymeric chains in the crystalline regions to give a single wider relaxation peak (Fig 4.6 f). Gaussian fitting has been done for peak present at 60^0C, to show the presence of two relaxation processes. For the sake of clarity, not all the high temperatures peaks have been fitted, but the merging of the peaks is clearly visible from the fig 4.6 (f). Wider distribution of relaxation times indicates more heterogeneity in the system because of the increase in interfacial region due to increased ceramic dispersion. At 40^oC, this peak is not observed in the composites as it is present at much lower frequency. It is not observed in PVDF also. This relaxation is of Maxwell-Wagner-Sillar (MWS) type [Ramajo et al (2008); Hedvig (1977)]. Maxwell Wagner Sillar polarization is always present in the multiphase systems having phases with different conductivities. In such materials, the charge accumulates at the ceramic particles - polymer interface. This gives rise to space charge polarization leading to increase in the value of ε' as well as the dielectric loss. As the dielectric permittivity of CCTO is much higher than that of PVDF matrix, unbounded charges form large dipoles at the polymer matrix – ceramic interface. The induced dipoles find it difficult to follow the alternation of the electric field giving rise to rapid decrease in ε' with frequency in the low frequency range.

Relaxation times, τ of the high frequency relaxation are determined using the relation $\tau = \frac{1}{2\pi f}$ where f is the frequency in cycles per second at the peak position in M" vs log f plots. Plots of log τ vs 1000/T for CCTO, PVDF, PVDF-10CCTO, PVDF-20CCTO and PVDF-50CCTO are shown in fig 4.7. These plots are linear in accordance with Arrhenius relationship given below:

$$\tau_{max} = \tau_o \exp(\frac{E_R}{kT}) \qquad (4.2)$$

where E_R is the activation energy of the relaxation process, τ_o is the pre- exponential factor, k is the Boltzmann constant and T is the absolute temperature. Values of the activation energy obtained from the slopes of these linear plots are given in Table 4.1. It is observed that the activation energy for α_c relaxation increases with increasing content of CCTO. This is due to increase in the stiffness of the composites with increasing content of CCTO.

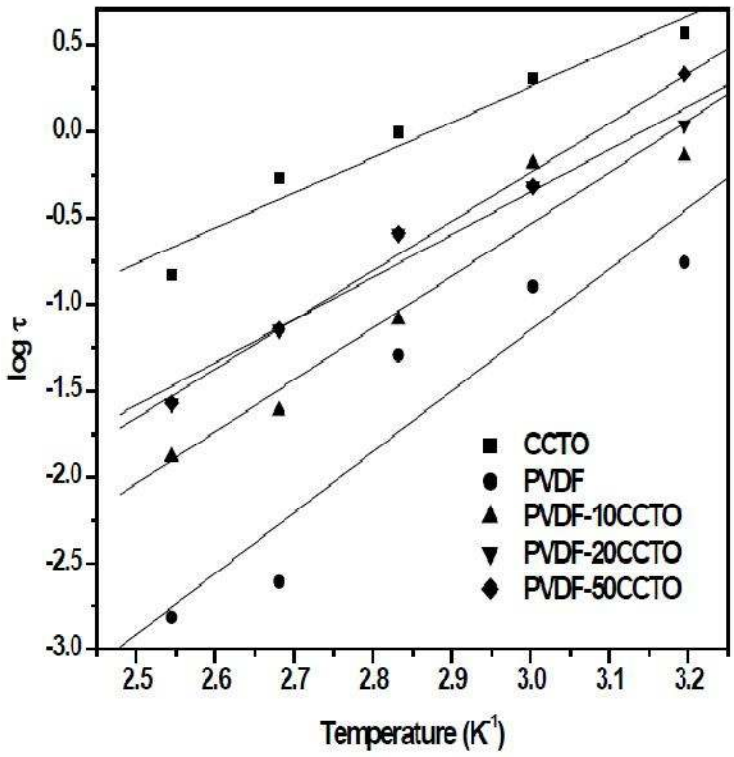

Figure 4.7 Log τ vs 1000/T plots for CCTO, PVDF, PVDF-10CCTO, PVDF-20CCTO and PVDF-50CCTO.

Table 4.1 Activation energy of dielectric relaxation, α_c, relaxation associated with molecular motion of the polymer chains in the crystalline regions of PVDF from M'' vs log f plots.

Sample	Activation Energy
CCTO	**0.41 eV**
PVDF	**0.70 eV**
PVDF-10CCTO	**0.70 eV**
PVDF-20CCTO	**0.72 eV**
PVDF-50CCTO	**0.78 eV**

It is also noted from fig 4.6 (c) that M'' peaks shift to low frequency with increasing content of CCTO. This is because of the restricted movement of the polymer chains as mentioned above. It is also in conformity with the increasing value of Young's modulus with increase in the content of CCTO as described in section 4.4.

Various models are used to predict the effective dielectric permittivity (ε' or ε_{eff} are the same) of the composites. The dielectric property of a biphasic dielectric mixture comprising of spherical crystallites with high dielectric permittivity and a matrix of low dielectric permittivity can be described by Maxwell's model [Maxwell 1954]. According to this model, the effective dielectric permittivity of the composite is given by

$$\varepsilon_{eff} = \frac{\delta_p \, \varepsilon_p \left(2/3 + \varepsilon_c/3\varepsilon_p\right) + \delta_c \, \varepsilon_c}{\delta_p \left(2/3 + \varepsilon_c/3\varepsilon_p\right) + \delta_c} \qquad (4.3)$$

where ε_c, ε_p, δ_c and δ_p are the dielectric permittivity of the CCTO, PVDF, the volume fraction of the ceramic and the polymer respectively. After substituting the values of ε_c, ε_p, δ_c and δ_p, the values of ε_{eff} obtained deviate much from the experimental values for all the wt fractions of CCTO under study (Fig 4.8).

In the case of Clausius-Mossotti model [Frolich 1949], it is assumed that the mixture of dielectric is composed of spherical crystallites dispersed in a continuous medium. The

effective dielectric permittivity (ε_{eff}) of the composite in this case is given by the following equation.

$$\varepsilon_{eff} = \varepsilon_p \left[1 + 3\delta \left(\frac{(\varepsilon_c - \varepsilon_p)}{\varepsilon_c + 2\varepsilon_p}\right)\right] \quad (4.4)$$

The predicted values of ε_{eff} using this model also deviate very much from the experimental values (Fig 4.8). This may be due to non spherical shape of CCTO particles in both the models as shown by SEM.

Lichtenecker's or logarithmic mixture rule is also used to predict the effective value of dielectric permittivity for the mixture [Nalwa 1995]. According to this model ε_{eff} is given by

$$\text{Log } \varepsilon_{eff} = \delta_1 log\varepsilon_1 + \delta_2 log\varepsilon_2 \quad (4.5)$$

Experimental results are significantly different from the predicted results using this model also (Fig 4.8). This is because Logarithmic law is applicable only when there is not much difference in the value of ε' of the dispersion medium and the dispersed phase. This is not true in the case of PVDF-CCTO composites. Therefore the experimental results do not match exactly with the values predicted by these models.

The effective medium theory (EMT) model [Rao et al (2000)] has been developed taking into account the morphology of the particles. According to this model, ε_{eff} is given by

$$\varepsilon_{eff} = \varepsilon_p\left[1 + \frac{f_c(\varepsilon_c - \varepsilon_p)}{\varepsilon_p + n(1-f_c)(\varepsilon_c - \varepsilon_p)}\right] \quad (4.6)$$

where f_c is the volume fraction of the ceramic dispersed, ε_c, ε_p and n are the dielectric permittivity of the ceramic, polymer and the ceramic morphology fitting factor respectively. The experimental values obtained are closest to the predicted values in this

case of all the models employed to predict the ε_{eff} values. The shape parameter n has been found to be 0.089.

All these models have the limitations that the chemistry of interfacial structure has not been taken into account and particles are assumed to be of spherical shape. Microstructure and microchemistry of the interfaces are also very important to determine the physical, mechanical and electrical properties of the composites.

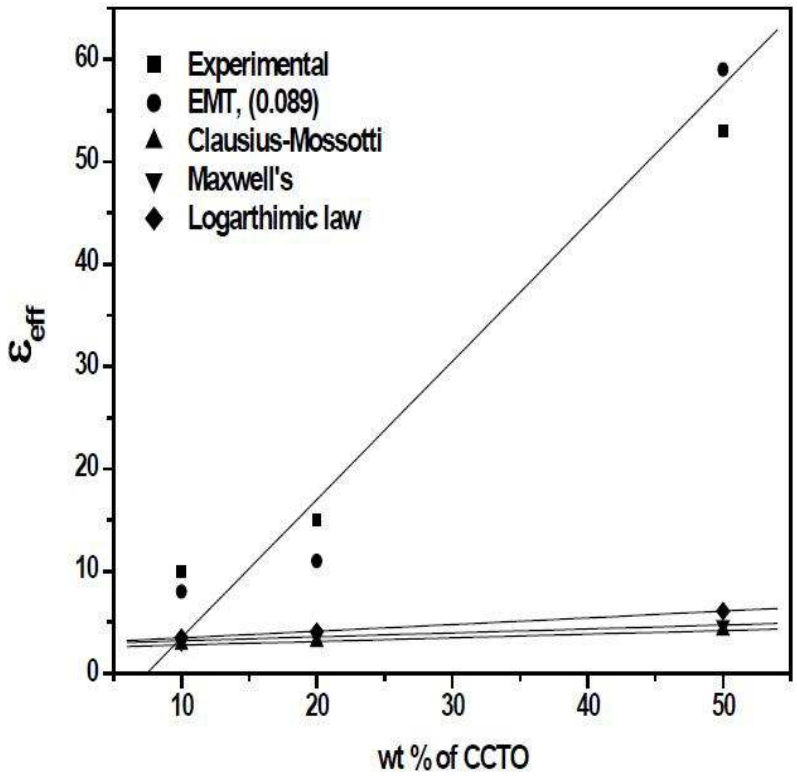

Figure 4.8 Variation of effective dielectric permittivity (ε_{eff}) measured at 100 Hz and 40^{o}C for PVDF-CCTO composites based on various models.

The temperature-dependent dielectric relaxation is explained by Havriliak-Negami (H-N) function [Windlass et al (2001); Mijovic et al (2006)]:

$$\varepsilon^{*} = -i\frac{\sigma_{dc}}{\varepsilon_0 \omega^{s}} + \varepsilon_{\infty} + \sum_j \frac{(\Delta\varepsilon)_j}{[1+(iw\tau_j)^{\alpha}]^{\beta}} \qquad (4.7)$$

where, σ_{dc} is dc conductivity, ω is the angular frequency, s is an exponent ($0<s \leq 1$), τ_j is the relaxation time of the j^{th} process, ε_0 is the vacuum permittivity, $\Delta\varepsilon$ is the dielectric strength of the j^{th} process and α and β are the shape parameters of the H-N function which define the symmetric and asymmetric broadening of the α_c relaxation peak in ε'' curve. Analysis of H-N function using WinFit software program of PVDF and PVDF-50CCTO composite have been given in Table 4.2 using deconvoluted H-N fits presented in (Fig.4.9). The exponent parameter, α represents the slope of the lower frequency side of the relaxation peak in ε'' curve. β is the asymmetry parameter which is calculated from the slope of higher frequency side of the same curve as α. The higher value of α for composites as compared to pure PVDF indicates a stretched relaxation over a wider range of frequencies whereas $0<\beta\leq1$ leads to asymmetrical broadening for the relaxation function. For $\beta=1$, the Debye-function is obtained. Asymmetry parameter β has a value of 1 for PVDF showing the symmetry of the spectrum. For the composites, β parameter has different values due to the dispersion of ceramics particles which creates heterogeneity in the system. For composites, the relaxation time (s) calculated from H-N fit decreases with increase in temperature. The composites exhibit lower relaxation time as compared to PVDF. Exact reason for this is not clear at present. With increase in the temperature, the relaxation time decreases in the composites. Lower value of relaxation time at higher temperature is because of the ease of relaxation at higher temperature due to increased mobility of the chains both for pure PVDF as well as composites.

Table 4.2 Fitting parameters for α_c relaxation as a function of temperature obtained from H-N fits.

Temp	PVDF, α	PVDF-50CCTO, α	PVDF, β	PVDF-50CCTO, β	PVDF, τ	PVDF-50CCTO, τ
40^0C	0.49	0.62	1	0.59	2.33E-2	2.12E-2
80^0C	0.53	0.63	1	0.62	1.45E-3	2.16E-3
120^0C	0.57	0.72	1	0.71	7.44E-4	8.18E-5

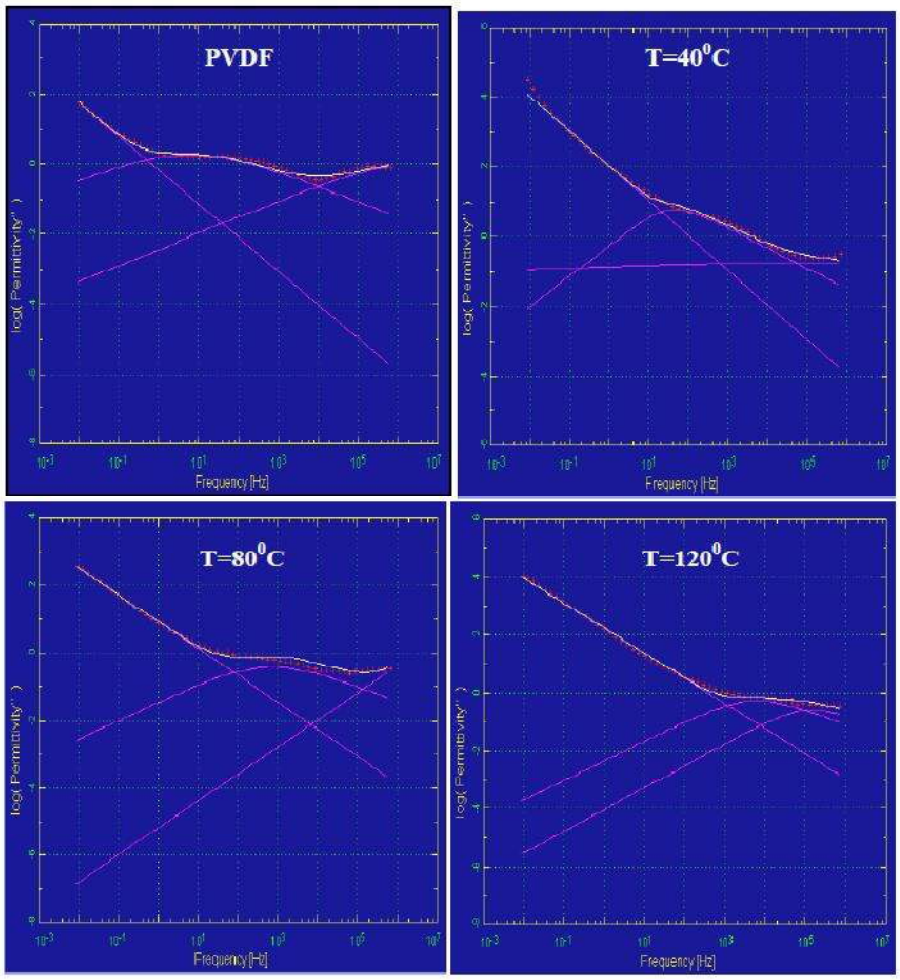

Figure 4.9: Dielectric loss in the frequency domain and spectrum was deconvoluted from H-N fits for PVDF-50CCTO composites at different temperatures.

4.6. Conclusion

- Composites containing 10, 20 and 50 wt % CCTO in PVDF have been prepared through melt extrusion process.

- XRD studies indicate that there is no change in the structure of either polymer or ceramic in the composites but the d-spacing changes with CCTO dispersion suggesting better interaction between PVDF and CCTO.

- Young's modulus increases significantly due to ceramic filler.

- Morphological studies reveal the homogeneous distribution of CCTO fillers in PVDF matrix.

- With addition of CCTO, there is substantial increase in the dielectric permittivity of PVDF matrix. Dielectric loss increases slightly with increasing temperature and decreases with increasing frequency. Composites exhibit two dielectric relaxations and the relaxation peaks shift towards higher frequency with increasing temperature.

- As the filler content increases in the PVDF matrix, M' value decreases. In the modulus spectroscopy, two dielectric relaxations have been observed in the composites. One relaxation occurring at low frequency is of Maxwell-Wagner-Sillar (MWS) type, while the other relaxation occurring in the intermediate frequency range is due to α_c relaxation associated with molecular motion of the polymer chains in the crystalline regions of PVDF.

- Temperature dependent dielectric relaxation has been worked out in details through H-N function. Debye type relaxation is observed in pure PVDF with $\beta=1$ while the stretched (broad) relaxation over a wider range of frequency has been observed in the composites suggesting asymmetric nature of the relaxation.